Isotropic−Nematic Phase Equilibrium and Phase Separation of κ-Carrageenan in Aqueous Salt Solution: Experimental and Theoretical Approaches

Ioannis S. Chronakis*,†,‡ and Mohamed Ramzi†,§,||

Physical Chemistry 1, Center for Chemistry and Chemical Engineering, Lund University, Box 124, S-221 00 Lund, Sweden; IFP Research, Swedish Institute for Fiber and Polymer Research, Box 104, S-431 22 Mölndal, Sweden; and Van't Hoff Laboratory of Physical and Colloid Chemistry, Utrecht University, Padualaan 8, 3584 CH Utrecht, The Netherlands

Received February 4, 2002; Revised Manuscript Received April 26, 2002

The behavior of chiral−nematic and isotropic phases of helical κ-carrageenan in aqueous solution of sodium iodide was compared with that of the anisotropic biphasic phase that contains both these phases. On the basis of birefringence, rheology, chemical analysis, average molecular weight, and polydispersity index measurements, we derived a number of characteristic differences as well as similarities between these phases, over a range of polysaccharide concentrations obtained by the dilution of each phase. For example, we assessed the critical concentration of an isotropic−anisotropic transition (C_i), the temperature of the anisotropic−isotropic phase shift during thermal heating−cooling cycles, and the viscosity changes due to the phase shift and due to the diminishing of the helical conformation. We also demonstrated how the different phases and their dilutions behave under the effect of shear and frequency of oscillation and how the viscoelastic properties vary in each phase and discussed the isotropic and anisotropic liquid crystal controlling behavior mechanisms. From a theoretical point of view, we propose to combine the wormlike chain model for semiflexible polyelectrolytes interacting via both hard-core and electrostatic repulsion to assess the concentration of isotropic−nematic transition, to assess the coexistence concentration range, and to determine the effects of charge by applying the effective diameter and a twisting effect.

Introduction

The carrageenans are linear, sulfated polygalactans extracted from various species of marine red algae, (i.e., *Eucheuma cottoni*, *Eucheuma spinosum*, *Gigartina acicularis*).[1,2] The primary structure is based on a repeating disaccharide sequence of 1,3-linked β-D-galactopyranose and 1,4-linked 3,6-anhydro-D-galactopyranose residues. κ- and ι-carrageenan are the two best known gelling varieties.

Rigid and semirigid macromolecules can form gels, but there is also a possibility to form ordered phases (nematic, chiral nematic, smectic, hexatic) or both gels and liquid crystalline phases.[3] The liquid crystalline phase is caused by restrictions on rotation, which in turn are caused by volume exclusion for the polymers of high axial ratios. Most experimental investigations on κ-carrageenan (KC) have dealt with conditions where gel formation or aggregations of the helices occur, therefore preventing the development of long-range liquid crystalline order. However, binding of iodide to the (negatively charged) KC helix increases the charge density, thus preventing aggregation and further gelation of the helices.[4,5] In fact, this was demonstrated for sodium iodide concentration of 0.1 M for polymer concentrations up to about 1 g/L. For higher values of sodium iodide concentration, aggregation does indeed take place, nevertheless, at a reduced extent.[6] The binding of iodide explains why the KC solutions require sodium iodide as a solvent to give a nematic liquid crystalline phase.[4] These solutions show a macroscopic phase separation into one anisotropic bottom phase and one isotropic top phase. The anisotropic phase is fluid, clear, and birefringent and has a chiral nematic structure.[4] It is a thermodynamically stable phase since it can be melted and reformed upon cooling; the melting of the nematic phase is fast (minutes) but the reverse transition is slower (5−6 days). Both the molecular weight of the polysaccharide and the ionic strength affect the phase boundaries of the nematic phase. Note that it was not possible to obtain a single-nematic phase by direct mixing, probably due to the polydispersity and to the presence of a small amount of ι-carrageenan contamination in the κ-carrageenan.[4,5] Surprisingly, ι-carrageenan, differing from κ-carrageenan only by an extra sulfate group, did not form a nematic phase.[4,5]

Indeed, the separation of a rodlike polymer into two phases, isotropic and anisotropic, above some critical concentration is well established experimentally and theoretically.[7−10] Several rigid polymers have been investigated, for example poly(*n*-hexylisocyanate)[11,12] and tobacco mosaic virus.[13] Mesophase formation in natural polysaccharides has

* To whom correspondence should be addressed at IFP Research, The Swedish Institute for Fiber and Polymer Research. Telephone: + 46 31706 63 00. Fax: + 46 31706 63 65. E-mail: ioannis.chronakis@ifp.se.

† Lund University.

‡ Swedish Institute for Fiber and Polymer Research.

§ Utrecht University.

|| Present address: Rhodia, Centre de Recherches d'Aubervilliers, 52 Rue de la Haie Coq, F-93308, Aubervilliers Cedex, France

10.1021/bm020015k CCC: $22.00
Published on Web 06/04/2002

been observed for many cellulosic derivatives,[14−16] for xanthan gum,[17−19] schizophyllan,[20] chitin,[21] scleroglucan,[22] and konjac[23] glucomannan. The concentration at which the liquid crystalline phase is formed depends on the persistence length of the polysaccharide. Xanthan, for instance, with a long persistence length (120 nm) forms a liquid crystalline phase at quite low concentrations (2−8 wt %).[19] Hydroxypropyl cellulose, with a short persistence length (between 5 and 10 nm), forms a liquid crystalline phase at much higher concentrations, around 30 wt % in a good solvent.[24] Recently it has been found that κ-carrageenan helix in 0.1 M NaI has a persistence length of 35.6 nm.[25]

Despite the progress made, the properties of liquid crystalline polymers are not fully understood yet theoretically. Liquid crystalline polymers (LCP's) can be approached theoretically with the basic model of the rigid rod.[7,8] However, the molecules are often semirigid or contain flexible spacers between the rigid groups that introduces more possibilities for the configuration.[26] Another important aspect that needs to consider is the effects of charge and ionic strength that biopolymers carry in aqueous solution.[27−29] From a theoretical point of view, electrostatic interactions can cause the rods to twist away from the parallel configuration with respect to each other and increase the hard-core diameter to a larger effective one, while the persistence length increases as well. Nevertheless, the viscoelastic properties of LCP's have been studied quantitatively in considerable detail over the recent years.[30,31]

In this investigation, the behavior of KC isotropic and nematic phases was compared with that of the anisotropic biphasic KC phase which contains both these phases (but were not macroscopically phase separated). Our approach was also extended to the analysis of the isotropic−anisotropic phase transition and coexistence concentration range of KC by the model proposed by Vroege and co-workers, that combine the wormlike chain model of semiflexible polymers extended to the charged case effect. Finally we discuss the isotropic and anisotropic controlling behavior mechanisms and summarize the similarities−differences in the structural and mechanical properties observed for these phases.

Theoretical Background

We elaborate here a simple model developed by Vroege and co-workers[27−29] to describe the formation of nematic liquid crystals for charged semiflexible polyelectrolytes interacting via both hard-core and electrostatic repulsions. It is possible to describe the result of charge by introducing an effective diameter and a twisting effect.

(1) The Effective Diameter. The electrostatic repulsion between the KC helices will results in an increase of the helix diameter. Instead of the "bare diameter", D, an effective diameter, D_{eff}, should be used, given by the expression[27]

$$\mathrm{D}_{\mathrm{eff}} = D\left[1 + \frac{\ln A' + C_{\mathrm{E}} + \ln 2 - \frac{1}{2}}{\kappa D}\right] \tag{1}$$

where the dimensionless parameter A' is given by

$$\mathrm{A}' = \frac{\Pi\Gamma^2 \mathrm{e}^{-\kappa D}}{2\kappa Q} \tag{2}$$

and Γ is a constant, C_{E} is Euler's constant, D is the helix diameter, κ^{-1} is the Debye screening length, and Q is the Bjerrum length

$$Q \equiv \frac{q^2}{\epsilon k_{\mathrm{B}} T} \tag{3}$$

(q is the elementary charge, ϵ is the supposedly uniform dielectric permittivity of the solvent, T is the temperature and k_{B} is Boltzman's constant).

(2) The Twisting Parameter. The twisting parameter describes the tendency of two charged rods to twist away from the parallel configuration to adopt a perpendicular orientation:

$$h = \frac{1}{\kappa D_{\mathrm{eff}}} \tag{4}$$

(3) Coexistence Concentrations (in Scaled Form). A well-known property of liquid crystals is that the anisotropic phase will coexist with a more dilute isotropic phase in a narrow concentration range. The scaled transition concentrations that denote the phases transition from an isotropic solution (of concentration C_{i}) to a nematic solution (of concentration C_{a}) vary with the twisting parameter h and are given by

$$C_{\mathrm{i}} = \frac{0.3588}{1 - \sqrt{x}} \tag{5}$$

and

$$C_{\mathrm{a}} = \frac{0.3588}{\sqrt{x} - x} = \frac{C_{\mathrm{i}}}{\sqrt{x}} \tag{6}$$

where $x = 0.8648 + 0.0991h$.

(4) Coexistence Volume Fractions. The coexistence volume fractions can be obtained from the equation

$$C_{\mathrm{i,a}} = \frac{\Pi}{4} P L D_{\mathrm{eff}} \frac{N_{\mathrm{L}}}{V} \tag{7}$$

where P is the persistence length, L is the contour length, and V is the volume of a solution of N_{L} very long polyelectrolyte.

For the isotropic and nematic phase, the real number densities can be derived from eq 7 by dividing by $(\pi/4)$-PLD_{eff}.

$$\left(\frac{N_{\mathrm{L}}}{V}\right)_{\mathrm{i}} = \frac{C_{\mathrm{i}}}{\frac{\pi}{4} P L D_{\mathrm{eff}}} \tag{8}$$

$$\left(\frac{N_{\mathrm{L}}}{V}\right)_{\mathrm{a}} = \frac{C_{\mathrm{a}}}{\frac{\pi}{4} P L D_{\mathrm{eff}}} \tag{9}$$

$(N/L)_{\mathrm{i}}$ and $(N/L)_{\mathrm{a}}$ can be expressed in mole of polymer/liter by multiplying by $10^{27}/6.022 \times 10^{23}$.

The real concentrations ρ_i and ρ_a can be obtained by multiplying by the molecular weight (see Appendix).

Experimental Section

Polysaccharide Purification. The κ-carrageenan was kindly donated from Sanofi Bio Industries, France (ref 12880). It was dissolved in 80 °C water and precipitated in cold 2-propanol, washed with a mixture of 40% water and 60% 2-propanol, and finally washed with pure 2-propanol. The precipitate was collected, and the 2-propanol was evaporated overnight. The dried κ-carrageenan was then dissolved in Millipore water (1.5 wt %). The solution was filtered through a 5 μm Millipore filter and ion-exchanged at 90 °C to the sodium form (cation-exchange resin, Dowex-50W, 50X8-100, Sigma). The resin was first converted to the H^+ form by elution with HCl and then to the Na^+ form by using NaCl. To obtain the desired average molecular weight, the κ-carrageenan was sonicated for 120 min which from previous studies in our laboratory correspond to a molecular weight of about 1.5×10^5,[4] (the actual weight-average molecular weight of the present sample is discussed in detail below). The solution was filtered through a 1.2 μm Millipore filter, to remove possible titanium particles fallen off from the sonicator. The resultant samples were then freeze-dried and stored.

Sample Preparation. Sample A. The κ-carrageenan sample (10 wt %) was hydrated in 0.1 M NaI at room temperature and then heated at 90 °C for 1 h with stirring. The hot polymer solution was allowed to cool overnight at 25 °C. The sample was then centrifuged for 72 h at 4000*g*, and the isotropic (top, sample A_{iso}) and the anisotropic (bottom, sample A_{nem}) phases were collected. The bottom phase observed between crossed polarizers was birefringent, grainy, and slightly colored. After centrifugation, the two phases remained separated without further changes. The KC concentrations reported below from sample A prepared after appropriate dilution of these two phases with 0.1 M NaI, (samples A_{iso} and A_{nem}). A small volume of a turbid precipitate was collected on the bottom of the tube after centrifugation, in addition to the isotropic and nematic phases mentioned. This was explained as a contamination of unknown composition and probably represents some macromolecular contamination of the natural polysaccharide.[5]

Sample B. A similar κ-carrageenan sample (6.5 wt % in 0.1 M NaI) was prepared as above: hydrated at room temperature and then heated at 90 °C for 1 h with stirring. The hot polymer solution was allowed to cool overnight at 25 °C. Then the sample was centrifuged for 72 h at 4000*g*, and the small volume of a turbid precipitate on the bottom of the tube was collected and discarded. The isotropic (top) and the anisotropic (bottom) phases were collected, and mixed again and then heated at 90 °C for 30 min while stirring. This sample, sample B_{biph}, refers to the biphasic mixtures before separation and contains both isotropic and nematic phase. Sample B_{biph} was diluted using 0.1 M NaI at nominal concentrations of 5, 4, and 2 wt %. Part of the sample B_{biph} was then centrifuged again for 72 h at 4000*g*, and the isotropic (top, sample B_{iso}) and the anisotropic (bottom, sample B_{nem}) phases were collected. Both phases were diluted with 0.1 M NaI at nominal concentrations of 5, 4, and 2 wt %. For the MW determination samples in solution form were prepared with the following characteristics: 4 wt % sample B_{biph}, 4 wt % sample B_{iso}, and 4 wt % sample B_{nem}. These samples were prepared from the dilution of 6.5 wt % sample B_{biph}, sample B_{iso}, and sample B_{nem}, respectively, using 0.1 M NaI. κ-Carrageenan concentrations are given as weight percent (wt %). Millipoore water was used throughout.

Table 1. Weight Average Molecular Weight (M_w) and the Polydispersity Index (M_w/M_n) of the Biphasic Sample (Sample B_{biph}), the Equilibrium Phases (B_{iso} and B_{nem}) of κ-Carrageenan (4 wt %) and the κ-Carrageenan Dry Powder

sample B-biphasic (4 wt %): $\langle M_w \rangle$ =117 000	$\langle M_w \rangle / \langle M_n \rangle = 1.87$
sample B-isotropic (4 wt %): $\langle M_w \rangle$ = 104 000	$\langle M_w \rangle / \langle M_n \rangle = 1.95$
sample B-nematic (4 wt %): $\langle M_w \rangle$ = 129 000	$\langle M_w \rangle / \langle M_n \rangle = 1.79$
κ-carrageenan powder: $\langle M_w \rangle$ = 113 000	$\langle M_w \rangle / \langle M_n \rangle = 1.85$

Average Molecular Weight and Polydispersity Index. The average molecular weight (M_w) and the polydispersity index (M_w/M_n) of κ-carrageenan samples were done by SEC with RI detector, kindly offered by CPKelco, Copenhagen Pectin A/S (Lille Skensved, Denmark). The weight-average M_w and the polydispersity index, found as average values from double runs, were presented in Table 1. Interestingly, the M_w values of the biphasic, isotropic, and nematic samples, and even more so the M_w/M_n values, are so close as to consider the difference among them as statistically insignificant. In fact $(M_w)_{avg} = 115\,800 \pm 10\,400$ (i.e. 9%). The above values are relative to a κ- and ι-carrageenan calibration set containing seven broad MW standards with known $\langle M_n \rangle$ and $\langle M_w \rangle$. The M_w range of calibration was 17 000−810 000. The samples were diluted to a concentration of about 0.5 mg/mL with 100 mM ammonium nitrate buffer, pH 9.7 (eluent) prior to injection. The run temperature was 60 °C (temperature well above the helix−coil transition temperature). Two columns (Shodex OHpak KB-806 M, 8 × 300 mm) and one precolumn (Shodex OHpak KB-G, 5 × 50 mm) were used, with a flux of 1.2 mL/min.

Chemical Analysis. Elemental analysis was performed by Mikro Kemi AB, Uppsala, Sweden. Carbon and sulfur were determined by catalytic oxidation at elevated temperature (1800 °C) in a controlled He/O_2 atmosphere, followed by gas chromatography to separate the different oxides (the so-called "Carlo Erba" method). Na and I analysis was performed by Analyslaboratoriet AB, Lund, Sweden. Sodium was determined by flame atomic absorption spectrometry, ionization suppression by addition of 2000 ppm of cesium to samples, and standards. Iodide was determined by spectrophotometric iodometric microtitration. The results were presented in Table 2.

It is notable, from Table 2, that the ratio of Na to I for the 5 wt % B samples is 0.412 and 0.385, respectively (mean = 0.398). The theoretical value for a 0.1 M NaI solution is 0.181. However, if the sodium ions stemming from the polysalt are properly taken into account, their concentration is [50 g/L]/[408 g/mol] = 0.123 M. Then, the theoretical Na/I weight ratio is 0.404, which compares in an excellent way with the mean of the two experimental values, i.e. 0.398.

Table 2. Elemental Analysis of the 2 wt % Biphasic Sample (Sample B_{biph}) and the Equilibrium Phases (B_{iso} and B_{nem}) of 2 and 5 wt % κ-Carrageenan Dissolved in 0.1 M NaI (Average of Three Measurements)

	contents (wt %)			
phase	C	S	Na	I
2 wt % B_{biph}	0.600	0.145		
2 wt % B_{iso}	0.600	0.146		
2 wt % B_{nem}	0.633	0.140		
5 wt % B_{iso}			5.33	12.95
5 wt % B_{nem}			5.24	13.60

This point is also important with respect to the calculation of the Debye length.

Rheological Measurements. Rheological measurements were performed on a Carri-Med CSL100 controlled stress rheometer (TA Instruments, Surrey, U.K.) using cone−plate geometry (40 mm radius, 40°, and 60 mm radius, 52°). The solutions were loaded on the platen of the rheometer and the storage modulus (G'), loss modulus (G''), tan δ, and complex viscosity (η^*) were recorded as a function of oscillation frequency. The strain applied (1%) was well within the linear region. The measurement was then followed by steady-state measurements. All measurements were performed at 25 °C except otherwise stated. The periphery of the sample was coated with silicone oil to minimize loss of solvent or absorption of atmospheric moisture.

Results and Discussions

Birefringence. The samples diluted from the isotropic upper phase sample A_{iso} (9−0.5 wt %) were lacking any birefringence under cross polarized light and flowed easily. In contrast, the dilutions from the anisotropic bottom phase sample A_{nem} (9−0.5 wt %), were optically isotropic up to 4.5 wt % and anisotropic from 4.99 wt % and beyond. Isotropic phases were not obtained after centrifugation (4 days) of the anisotropic samples at a temperature range from 25 to 40 °C. The anisotropy disappeared when the polysaccharide phases heated above ∼60 °C.

Samples B_{iso} were lacking any birefringence at the whole concentration range (2−6.5 wt %). Similarly no birefringence was obtained for the samples B_{biph} and sample B_{nem} up to a concentration of 4 wt %. However these samples were anisotropic (birefringent) at 5 wt % and beyond that concentration. Flow birefringence was observed at the 5 wt % for B_{biph} and B_{nem} samples, manifested by flashes of light when the tube was shaken between crossed polarizers. The critical concentration of ∼5 wt % for mesophase formation of KC is in accordance with the previous studies by Piculell's group.[5,32] Note that all the above solutions are stable over long times (many months). In what follows we use the word "rigid rods" to indicate the liquid-crystals of KC; in our system a substantial evidence which suggests the presence of such "rigid rods" is the different response of the anisotropic samples under polarized light, low amplitude of oscillation, and shear rate, in comparison with the isotropic phase behavior.

κ-Carrageenan Sample A. Low Amplitude Oscillatory Behavior. Figure 1a illustrates the frequency dependence of the 2.95 wt % isotropic KC obtained after the dilution of the nematic solution sample A_{nem}. The mechanical spectrum is typical of an entangled polysaccharide solution with weak cross-links;[33,34] $G' < G''$ at low frequencies whereas a crossover occurs at higher frequencies. A weak gellike behavior was observed for the anisotropic samples 4.99 and 5.22 wt % (Figure 1b,c); G' dominates G'' at high frequencies but both moduli still show significant frequency dependence. Both moduli, however, were progressively *lower* as the concentration increased from 4.99 to 5.22 wt %. Increasing further the concentration of the anisotropic phase, a significant *decrease* in storage and loss moduli was observed. A representative example is shown in Figure 1d for the 6.95 wt % sample where G'' is always higher than G' and both moduli were highly frequency dependent and increase in a parallel manner with increasing frequency of oscillation. Moreover, a simple way to address some dynamic aspects of the polysaccharide is to look the frequency of intersection of elastic and loss moduli. We can regard this crossover frequency as a measure of an effective junction lifetime. The crossover frequency of G' and G'' moved to lower values as the polysaccharide concentration was increased (for instance at 6 and 0.1 Hz for 2.95 and 4.99 wt %, respectively). However, for the anisotropic 5.2 wt % sample A_{nem}, the crossover moved to a higher frequency (at ∼1 Hz), and this sample showed a 10 times shorter relaxation time than the 4.99 wt % sample. No crossover was found for the higher anisotropic concentrations (between 6 and 9 wt %).

The elastic modulus G' allows us to compare the moduli with frequency of oscillation and to correlate these data with the Newtonian viscosity and shear flow results presented below. In Figure 2, the elastic modulus G' of the nematic sample A_{nem} dilutions were plotted as a function of the polysaccharide concentration at different frequencies. When the concentration of the isotropic samples (from the dilutions of sample A_{nem}) was increased, the elastic modulus rose steeply up to about 4.5−5 wt % (C_i), and then it began to drop in the anisotropic phase area. Further the modulus was kept almost constant well within the chiral nematic phase up to about 9 wt %. This behavior is typical of a liquid crystal: the elasticity decreases when there is a very high degree of alignment in the polymer as the elastic behavior depends sensitively on constraints at each contacting points between rods.[35,36] Note that the KC concentration C_i, where the maximum modulus was obtained, can well be compared with the concentration where birefringence starts to develop as obtained by visual observations. Obviously, this concentration presents the isotropic−anisotropic transition, where the anisotropic phase begin to appear, but does not mark the transition from the isotropic to a completely nematic phase.

In this work, we have also tried to separate and compare the structural behavior of the isotropic phase as affected by variables such as the frequency of oscillation and the shear rate. The frequency sweep measurements from the dilutions of the isotropic sample A_{iso} showed samples with a typical solution-like behavior and a typical example is shown in Figure 3. Both moduli were highly frequency dependent and increased progressively with increasing frequency of oscil-

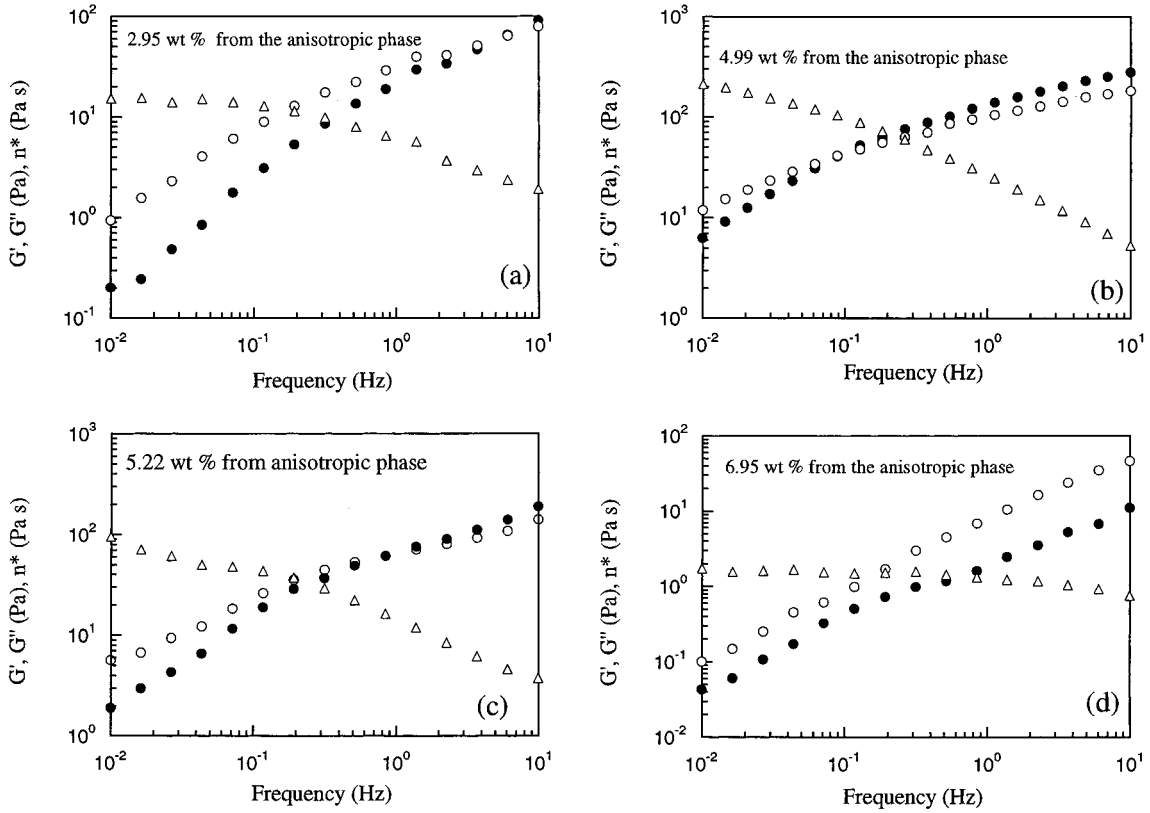

Figure 1. Frequency dependencies of G' (●), G'' (○), and complex viscosity η^* (△) obtained from oscillatory rheological measurements, for the dilutions of the nematic sample A_{nem} of κ-carrageenan in 0.1 M NaI. Key: (a) 2.95 wt % (isotropic); (b) 4.99 wt % (anisotropic); (c) 5.22 wt % (anisotropic); (d) 6.95 wt % (anisotropic). 25 °C, 1% strain.

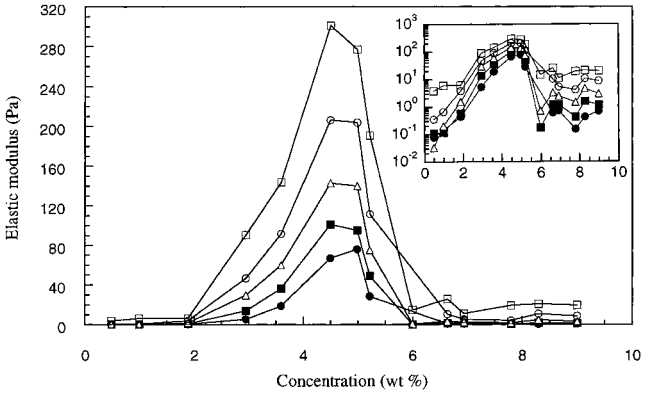

Figure 2. Variation of the elastic modulus G' as a function of κ-carrageenan concentrations in 0.1 M NaI of sample A_{nem} measured at various frequencies: (●) 0.26, (■) 0.52, (△) 1.37, (○) 3.72, and (□) 10 Hz. The concentrations were prepared after dilution of the nematic solution phase, sample A_{nem}. The insert graph shows the same data in a logarithmic scale. 25 °C, 1% strain.

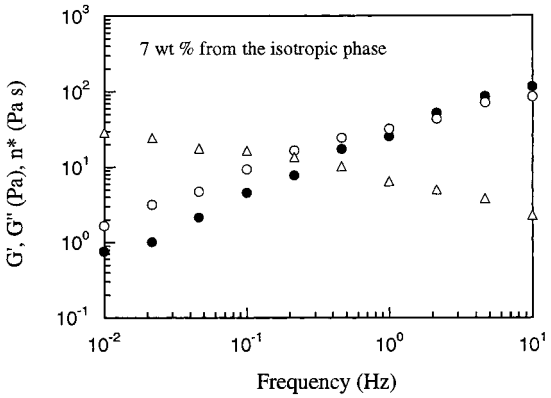

Figure 3. Frequency dependencies of G' (●), G'' (○), and complex viscosity η^* (△) obtained from oscillatory measurements, for 7 wt % κ-carrageenan in 0.1 M NaI from the dilution of the isotropic phase sample A_{iso}.

lation. The isotropic samples A_{iso} below 5 wt % showed very low viscosity, and we were unable to examine them under low amplitude oscillation with our rheometer.

Steady-State Shear Behavior. Following an examination of the rheological response at low deformation, we now examine our phases at large deformations under shear. Steady-shear viscosity measurements at 25 °C were made over a range of shear rates for the dilutions of the nematic phase sample A_{nem} as is shown in Figure 4. Interestingly, the viscosity of the solutions was decreased beyond 5 wt % of the KC. A Newtonian plateau, for about 3 orders of magnitude, where the viscosity is almost constant with shear rate and a shear thinning region could be attained for the KC concentrations up to 3 wt %. The Newtonian region, however, was not attained experimentally for the systems between 3.5 wt % and up to the concentration where the viscosity starts to decrease (∼5 wt %), which all show a pronounced shear thinning behavior and a strong shear rate dependency on the viscosity. Higher KC concentrations (above 5 wt %) have lower viscosity, while a Newtonian region and a shear-dependent region were observed. The high shear dependence is more noticeable for the liquid crystalline solutions and is due to the orientation of the molecular rods. It is notable as well that the flow curves of the different concentrations of the anisotropic solutions intersect at high shear rates, in accordance with other experimental and

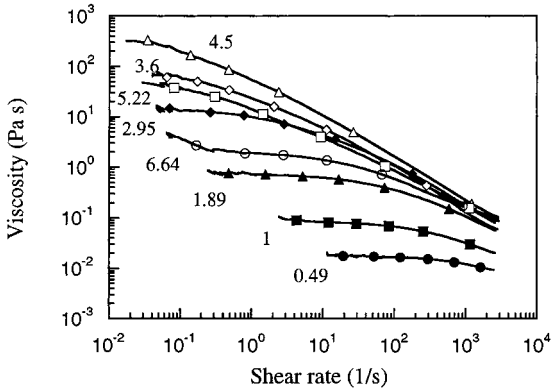

Figure 4. Steady-state flow curves at 25 °C of κ-carrageenan concentrations in 0.1 M NaI obtained after the dilution of the nematic solution sample A_{nem}: (●) 0.49, (■) 1, (▲) 1.89, (◆) 2.95, (◇) 3.6, (△) 4.5, (□) 5.22, (anisotropic), and (○) 6.64 wt % (anisotropic).

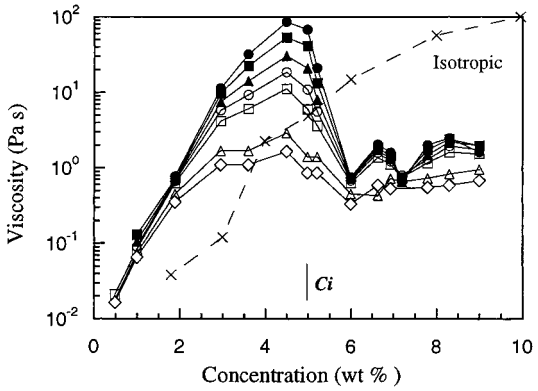

Figure 5. (a) Viscosity of the nematic solution sample A_{nem} as a function of κ-carrageenan concentration in 0.1 M NaI at different shear rates at 25 °C: (●) 0.5, (■) 1, (▲) 2.5, (○) 5, (□) 10, (△) 50 and (◇) 100 s^{-1}. Variation in the Newtonian viscosity (×) as a function of the isotropic κ-carrageenan concentrations of sample A_{iso} in 0.1 M NaI at 25 °C.

theoretical observations for the liquid crystals.[35] Reversible shear thinning behaviors were obtained for all the samples.

In Figure 5, the viscosity of the sample A_{nem} at different shear rates was plotted as a function of KC concentration. When the concentration in the isotropic phase was increased, the viscosity rises steeply up to about 4.5 wt %, and then it begins to drop as the concentration increased further at the anisotropic phase area. The viscosity was kept almost constant well within the anisotropic phase up to about 9 wt %. This behavior is in accordance with the trends of the concentration dependence of the elastic moduli (Figure 2). The response of reaching a viscosity maximum, which then falls sharply is a typical response of lyotropic mesophases.[18,30,35,37−39] As the concentration of rods in the isotropic phase increases, rotation is hindered sterically and the viscosity increases. At some critical concentration, the polysaccharide rods align to lower their free energy, where each rod now has less rotational hindrance and the increased alignment lowers the viscosity. Actually, the viscosity decrease after this maximum is quite significant; for example about 99% reduction when the concentration of the sample A_{nem} was increased from 4.5 to 6 wt % at a shear rate of 0.5 s^{-1}. This dependency was much lower in the case of xanthan polysaccharide[18] and for PBLG.[40] For instance a viscosity reduction of 60% was observed on increasing PBLG

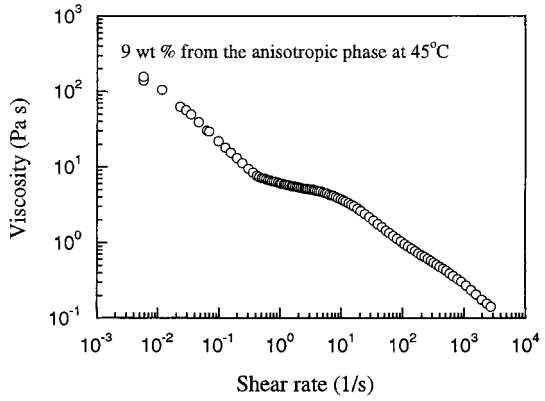

Figure 6. Steady-state flow curve at 45 °C of 9 wt % (anisotropic) κ-carrageenan sample A_{nem} in 0.1 M NaI.

concentrations from 19 to 30% in 1,4-dioxane.[40] We also observed substantial decrease of the viscosity at the critical concentration (C_i, ~5 wt %); for example by almost 2 orders of magnitude when the shear rate was increased from 0.5 to 100 s^{-1} (Figure 5). The viscosity now between 6 and 9 wt % of the anisotropic KC phase was approximately similar at the various shear rates. Very likely the shear orients the nematic phase in the shear direction throughout the sample as if the various domains coalesced into a single one. It appears, therefore, that the anisotropic KC phase has a "homogeneous" structure and orientation, and seem to be in a monodomain state. There is no creation of flow-induced defects, since G' and viscosity are constant in the nematic state, and viscosity is Newtonian at low shear rates. This is an interesting characteristic and it opens the way to study the rheology (first normal stress difference, start-ups, relaxation, interrupted start-ups) in a monodomain state.

Figure 5 illustrates as well the Newtonian shear viscosity for the isotropic sample A_{iso} dilutions. The viscosity was increased progressively upon the increase of the isotropic KC concentration. Clearly, the viscosity of the isotropic samples A_{iso} was lower than the viscosity of the isotropic samples obtained from the samples A_{nem}. However, beyond 5 wt % the viscosity of the isotropic solutions from sample A_{iso} was higher than that the corresponding obtained from the dilution of the nematic samples by 1 to 2 orders of magnitude.

Returning again to the behavior of the viscosity with shear rate, we detected another region of shear thinning at low values of shear rate. Thus, the curve of the viscosity vs shear rate exhibited three flow regions, a shear thinning at low shear rates, a constant viscosity region and a final shear thinning behavior. This region at low shear rates was more distinct when the flow curves were examined at a temperature higher than the ambient and close to anisotropic−isotropic transition temperature (see below). A typical example is shown in Figure 6 for the 9 wt % KC from sample A_{nem} at 45 °C. The slope (logarithm of viscosity vs logarithm of shear rate) in this region was 0.71. Such steady-state region is known as *region I* and is another characteristic property of the liquid crystalline polymers observed in a variety of systems.[41−43] This is thought to be a universal behavior caused by a defect ridden structure that is often denoted as "texture" or "domain structure".[43] The reason we more

clearly observed the flow region I at a temperature higher than the ambient is not clear. Throughout region I and part of the next region (region II), the polydomain structure is preserved despite the flow, while no significant net orientation is induced by the flow process.[42] Therefore, the most likely explanation could be the effect of temperature on the persistence length of the liquid crystals, as it is well-known that the persistence length is directly affected by the variation of the temperature.[31] The relation between the multidomain structure of KC and temperature needs further attention.

Cox−Merz Rule. We will now concentrate on the differences between the oscillatory and steady state shear properties. Essentially the only information that we have used is the simple Cox−Merz rule. For ordinary polymers the empirical rule of Cox−Merz applies well, without a full theoretical explanation. According to this, for equal values of frequency of oscillation and shear rate, the complex viscosity is equal to the steady shear viscosity. However, this is not the case for liquid crystalline polymers where the steady-state values drop below or rise above the oscillatory values.[44−46] These peculiarities are intrinsic to the nematic phase of the polymers. The steady shear viscosity of the anisotropic κ-carrageenan is substantially lower than the corresponding dynamic complex viscosity probably as a consequence of shear-induced orientation (Figure 7 a, b). Similar behavior was observed for xanthan and hydropropylcellulose as well for most other LCPs.[44,45,47] The deviation from the Cox−Merz rule suggests that the longest time scale probed in the dynamic experiments is too short to observe orientation and flow of the anisotropic KC phase domains. However, the steady shear viscosity of the isotropic phases (below C_i) superimpose closely with the dynamic viscosity at all shear rates (Figure 7c). This argues that the intermolecular interactions are purely topological entanglements.

Temperature Dependence of Viscosity. The viscosity of KC rigid rods depends not only on the shear rate but also on the temperature due to the temperature-dependent helix−coil equilibrium since only the helical conformation is capable of forming a nematic phase. The temperature increment has two effects: one is the shift in the phase volume diminishing the nematic phase and increasing the isotropic one (indeed the excluded volume is the driving force for the nematic−isotropic phase transition) and the other effect is of course the decrease in the helical content. Figure 8 shows the viscosity as a function of temperature for isotropic and nematic KC solutions from the dilution of the sample A_{nem}. The viscosity of isotropic κ-carrageenan (2.95 wt %) decreased as expected with heating and then above the helix−coil transition it remains unchanged. This behavior was also observed for the lowest anisotropic concentration of 4.99 wt %. On the other hand, the viscosity of anisotropic phases 6.5 and 9 wt % *increased* steadily with the temperature up to a nematic−isotropic transition and then it dropped to a lower value when the temperature increased further (Figure 8). This is a well-known rheological property of liquid crystals.[30] Obviously, the anisotropic phase exist over a broad temperature intervals from ambient temperature and beyond the viscosity maximum with significant viscosity changes but does not persist all the way up to the helix−coil transition. Note as well, that the temperature of anisotropic−isotropic transition was increased progressively as the concentration of the anisotropic phase was increased (see also below). The helix−coil transitions were in accordance with the transitions observed from previous oscillatory and calorimetric measurements.[34,48,49]

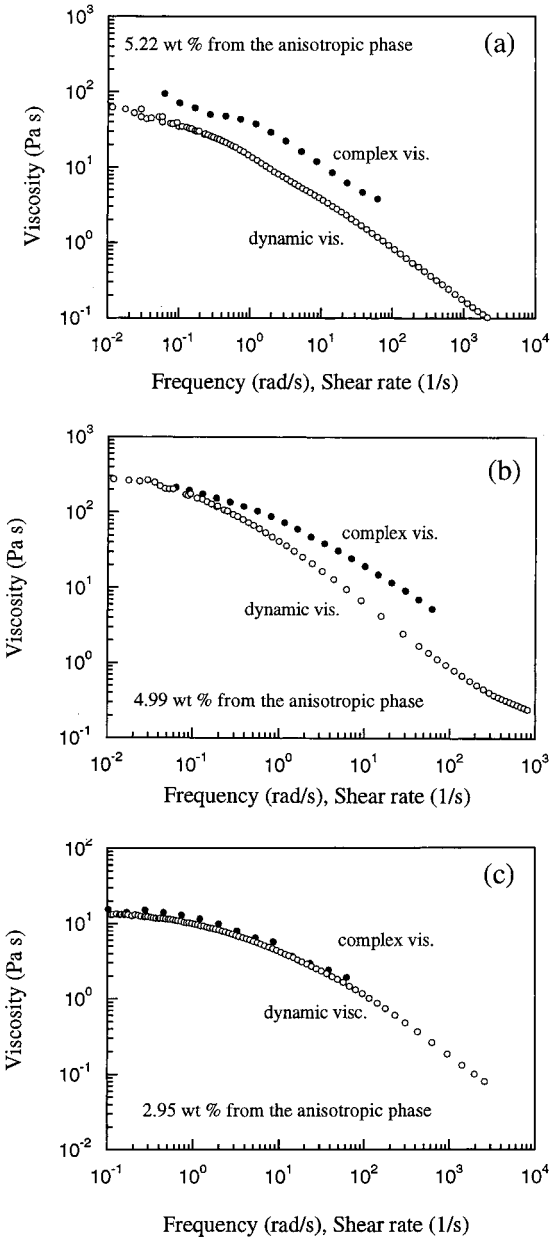

Figure 7. Testing of Cox−Merz rule for the nematic phase sample A_{nem} dilutions of κ-carrageenan in 0.1 M NaI: (●) complex viscosity η^*, and (○) steady shear viscosity η. Key: (a) 5.22 wt % (anisotropic), (b) 4.99 wt % (anisotropic), and (c) 2.95 wt % (isotropic). 1% strain, 25 °C.

κ-Carrageenan Sample B. To characterize further the lyotropic behavior of KC polysaccharide and confirm the above results, we have prepared a new sample B (that contains both phases which are not macroscopically phase separated, B_{biph}) and also two other samples B_{iso} and B_{nem} after centrifugation and separation of isotropic and anisotropic phases (see Experimental Section). Figure 9a shows the viscosity changes at different shear rates for the dilutions of 6.5 wt % sample B_{biph}. The behavior of the same sample

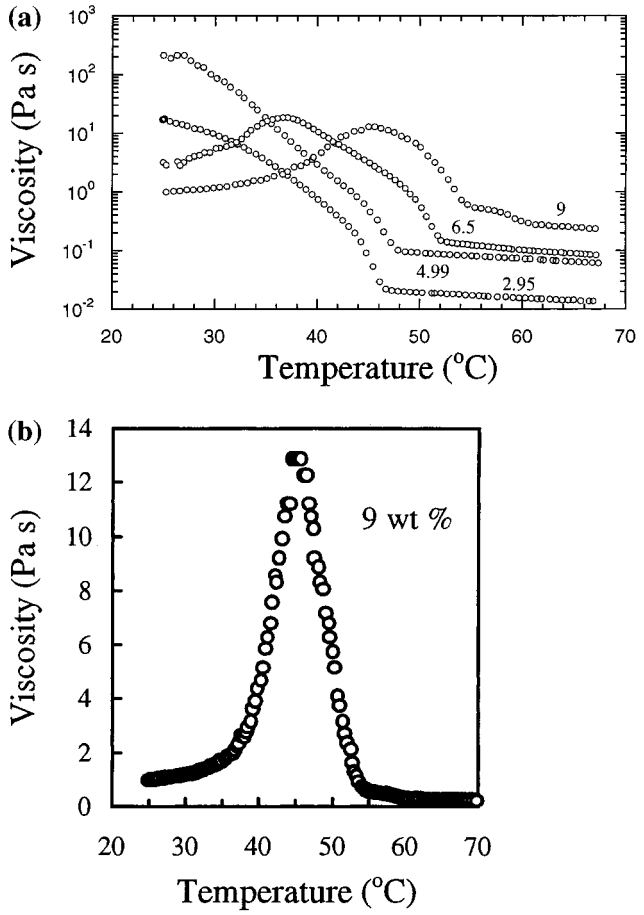

Figure 8. (a) Shear viscosity as a function of temperature for various concentrations of κ-carrageenan sample A_{nem} in 0.1 M NaI, 2.95 wt %: 8 Pa shear stress applied, initial shear rate of 0.5 s^{-1}; 4.95 wt %, 10 Pa shear stress applied, initial shear rate of 0.05 s^{-1}; 6.5 wt %, 15 Pa shear rate, initial shear rate of 1 s^{-1}; and 9 wt % 1.5Pa shear stress applied initial shear rate of 1.5 s^{-1}. (b) Shear viscosity as a function of temperature for 9 wt % sample in the linear scale. The heating rate was 0.2 deg/min.

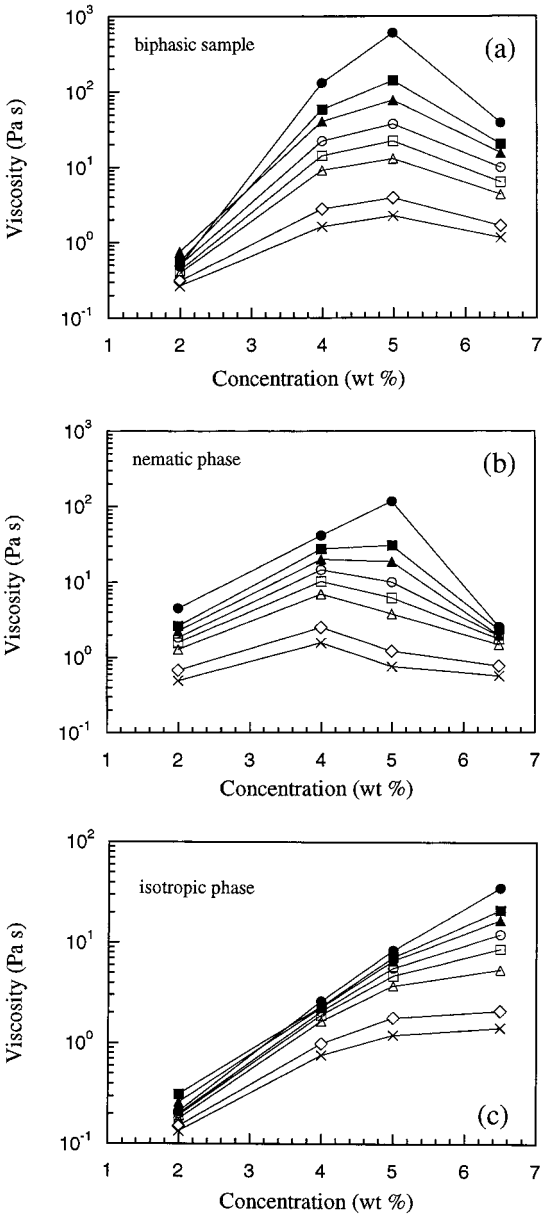

Figure 9. Viscosity of dilutions of κ-carrageenan phases in 0.1 M NaI as a function of concentration at different shear rates at 25 °C: (●) Newtonian viscosity and (■) 0.5, (▲) 1, (○) 2.5, (□) 5, (△) 10, (◇) 50, and (×) 100 s^{-1}. Key: (a) Biphasic solution B_{biph}; (b) nematic solution sample B_{nem}; (c) isotropic solution B_{iso}.

separated into isotropic and anisotropic phases and then diluted to various concentrations with 0.1 M NaI, samples B_{iso} and sample B_{nem}, respectively, is shown in Figure 9, parts b and c. Three conclusions can be drawn from the results: (i) The viscosity of the biphasic sample B_{biph} and the anisotropic sample B_{nem} rose progressively and steadily up to about 5 wt % where it suddenly dropped to a lower value. This concentration most probably denotes the transition from the isotropic phase to a coexistence phase that consists of both isotropic and nematic phases. In some way this could be confirmed from the same trends that the mixed sample B_{biph} demonstrate (B_{biph} cannot be a completely pure nematic at 5 wt %). (ii) For the concentration interval between 2 and 5 wt %, the nematic phase samples B_{nem} showed higher viscosity at all shear rates than the isotropic B_{iso} and the B_{biph} samples, while the sample B_{biph} has higher viscosity at all shear rates than the isotropic sample B_{iso}. (iii) Above the isotropic−coexistence critical concentration, the viscosity of the phases increased in the order $B_{iso} \gg B_{biph} \approx B_{nem}$. This is reasonable as we can imagine that, in a shear field, each domain may flow as a single "ensemble" of rods. The shear strain need to transport domains with respect to each other is small compared to the shear stress necessary to move far higher number of individual helices (as exist in the isotropic sample). These results are in agreement with the previous data illustrated in Figure 5 and similar conclusions could be obtained from the oscillatory elastic modulus (data, not shown here).

The effect of temperature on the viscosity changes of sample B (B_{iso}, B_{biph}, and B_{nem}) was also was evaluated (Figure 10). As discussed previously (Figure 8) the anisotropic samples undergo a nematic−isotropic transition where the viscosity was increased progressively up to a maximum value and then decreased steadily up to helix−coil transition. The maximum denotes two processes with an opposite sign: the loss of the nematic phase and then the gradual appearance of isotropic phase. Note that the temperature where the maximum viscosity observed (T_{max}) was not the same for the anisotropic samples; the B_{biph} sample showed

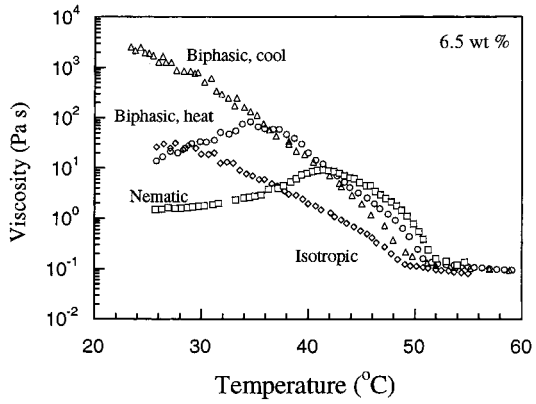

Figure 10. Shear viscosity as a function of temperature for 6.5 wt % κ-carrageenan sample B in 0.1 M NaI: Biphasic solution B_{biph}, both the heating (○) and the cooling (△) routes are shown; heating of the nematic solution sample B_{nem} (□); heating of the isotropic solution B_{iso} (◇). The heating rate was 0.2 deg/min.

a maximum viscosity at about 35 °C while for the sample B_{nem} it was at about 42 °C. The differences in the temperature of T_{max} between the biphasic sample and the nematic are most probably due to different liquid crystalline concentrations. For lower LC concentrations (as in the case of the biphasic sample), the sample is expected to have a lower nematic−isotropic transition temperature than the purely nematic phase. Furthermore, the helix−coil transition temperature was almost the same for both phases, B_{biph} and B_{nem}, while for the isotropic phase, it was slightly lower (by about 4 deg). Although our data from the elemental analysis show that roughly all phases have the same concentration, it was observed previously from ^{13}C NMR that the concentration of KC was only slightly higher (by ca. 0.6 wt %) in the nematic phase.[5] The relative intensities of the ^{13}C signals in the two phases also showed that the isotropic phase contained a larger fraction of coils than the nematic phase and this may explain such slight differences in the helix−coil transition. Interestingly, on cooling, the viscosity of the biphasic sample B_{biph} reached higher values at temperatures below the nematic−isotropic transition. This may originate due to the presence of an isotropic phase which has a higher viscosity (at the KC concentrations above C_i) than the fully anisotropic phases (Figure 9). Note that the rate at which the concentration of the helices was increased (i.e., the cooling rate) is also known to affect the ability of the system to reach its equilibrium state.[32] Despite the fact that our cooling rate is relative slow (0.2 deg/min), this may still produce an isotropic phase that is not in an equilibrium state with the nematic one (as was observed before heating the biphasic sample). Further work is needed in order to examine to what extent the viscosity changes and the equilibrium state depend on the rate at which the coil−helix transition is passed, what the kinetics of the formation of isotropic and nematic phases are, and how the increase of the helical concentration can change the conditions for the formation of the nematic phase.

The effect of temperature on the birefringence (under cross polarized light) of sample B was also evaluated (namely the samples 5 wt % B_{nem} and 6.5 wt % B_{biph}, B_{iso}, and B_{nem}). The sample 5 wt % B_{nem} was anisotropic and shear birefringent (on shake) at 32, 34, and 36 °C. At 38 °C, the sample was isotropic but still shear birefringent (the permanent birefringence was gone) and was a little clearer after standing at 38 °C for 15 min. Similar to this was the behavior of the sample at 40 °C. At 42 and 44 °C the sample 5 wt % B_{nem} started to flow although the sample was thick and clear and showed shear birefringence. In the temperature range between 46 and 50 °C, the sample was still shear birefringent and viscous, while at 53 °C the shear birefringence was gone and the sample flowed. Regarding the sample of 6.5 wt %: at temperatures between 32 and 40 °C, both B_{biph} and B_{nem} were permanent birefringent. Some birefringence was lost as the temperature was increased (from 32 to 40 °C), but they were still fully anisotropic. At 42 °C B_{biph} started to flow and was almost clear and shear birefringent on shake, while B_{nem} was still more shear birefringent (but not permanent birefringent) and a bit more hazy than B_{biph}. At 44 °C, B_{nem} flowed more easily, was totally clear, and still shear birefringent as also was the B_{biph}. A similar behavior was observed at temperatures between 44 and 46 °C. At 46 °C, B_{iso} started to flow easily. At 48 °C 6.5 wt % samples B_{biph} and B_{nem} still show some shear birefringence with the nematic solution B_{nem} observed to be more viscous. At 50 °C, 6.5 wt % sample B_{biph} and the respective B_{nem} were still viscous and shear birefringent. At 53 °C, the shear birefringence has disappeared for both 6.5 wt % B_{biph} and B_{nem}, respectively, and started to flow easily. Note that the nematic phase disappeared gradually as the temperature was increased, while after the disappearance of the birefringence some nematic phase may still remain as denoted from the shear birefringence of the anisotropic solutions.

Further Considerations

Well-established theories predict the formation of an anisotropic phase as the concentration of rodlike polymers increases. The anisotropic phase will coexist with a more dilute isotropic phase in a narrow concentration range where the solution will be biphasic.[7,8] As the concentration increases further, the fraction of anisotropic phase increases at the expense of the isotropic phase without, however, changing the concentration in each phase until the solution becomes fully liquid-crystalline. In previous studies, for example for xanthan solutions, separation of the anisotropic and isotropic phases was not successful and only both coexisting phases were investigated.[47,50] In our KC system, on the other, we were able to separate the nematic phase from the isotropic phase and investigate the rheology of both phases. We do not manage to isolate any isotropic phase at the coexistence region (between the C_i and C_a) even after extensive centrifugation at 40 °C. Previous studies from Piculell's group have also discussed the difficulties to separate dilute isotropic phase from the nematic one. Nevertheless, the efficiency of centrifugation to provide a complete separation of the isotropic and the nematic phases was confirmed by NMR.[32]

The first appearance of the nematic phase is at C_i, which corresponds to the critical concentration (weight fraction) for formation of the anisotropic phase. Our rheological experiments and the onset of birefringence locate C_i at 5 wt % for KC in 0.1 M NaI. If we apply the theoretical model

discussed previously by Vroege and accept that the hard-core diameter of KC is of 14 Å (based on the fact that the radius of the helix of KC in 0.1 M NaI is 7 Å as found from neutron and X-ray scattering measurements, Ramzi et al., unpublished), the effective diameter was calculated to be 37.81 Å (see Appendix). Considering that the κ-carrageenan in 0.1 M NaI has a persistence length of 35.6 nm,[25] we estimate the weight fraction for the isotropic−nematic transition at 4.7 wt % − 4.8 wt %, respectively (see also Appendix). Indeed, these values are in the close agreement with the value that we found experimentally.

Theoretically, the biphasic region is predicted to be quite narrow, $C_a/C_i = 1.14$, for $L \gg p$.[27] The coexistence concentrations ratio for our KC was found to be at $C_a/C_i = 1.02$ (see Appendix), close to the theoretical predictions. At this point it is useful to mention that, as pointed out by Vroege, the phase transition concentrations are clearly dependent on charge, while the properties of the nematic phase transition are not in contrast to the result for rodlike polyelectrolytes. Furthermore, theoretical work such as Mathesson's theory predicts that the fully crystalline phase can be deduced from the concentration corresponding to the minimum viscosity, which is about 6 wt % in our system.[51] Finally, in principle, deviations from the theoretical calculations, at least in part, could originate from the polydispersity of the natural polysaccharide that certainly influences the phase equilibrium and from the contamination of impurities (such as ι-carrageenan that do not form a nematic phase).

Moreover, it is not evident why the isotropic phase solutions have lower viscosities than that of the isotropic solutions obtained from the dilution of the nematic phase (i.e., Figures 5 and 9, for viscosity below C_i). By ^{13}C NMR, it was shown that both nematic and isotropic phase contain a small fraction of carrageenan chains in the coil conformation at room temperature, in agreement with optical rotation experiments performed in dilute solutions.[32] This is not unreasonable considering that a degradation by sonication could produce a significantly larger fraction of very short chains that did not transform into the helical conformation. Moreover, the relative intensities of the ^{13}C signals in the two phases indicate that the isotropic phase contains a larger fraction of coils than the nematic phase (a trend in qualitative agreement with theoretical considerations). It is doubtful, nevertheless, that this effect could be a large reason to explain such large differences in viscosity. Both the molecular weight and the polydispersity index cannot also explain such differences; interestingly, isotropic and nematic phases have similar M_w and M_n, as has also the biphasic sample that contains these phases. From elemental analysis, it was also confirmed that isotropic, anisotropic, and biphasic samples all have roughly the same KC concentration (Table 2) as expected for an isotropic−anisotropic phase equilibrium in a good solvent.[7,8]

Concluding Remarks

By comparing isotropic, chiral−nematic, and biphasic KC phases we assessed their similarities−differences. The *similarities* we have observed are as follows: (i) Both biphasic phase and chiral nematic phase show by birefringence and rheology the same critical concentration of an isotropic−anisotropic transition (at 5 wt %). (ii) A maximum in the viscosity at the anisotropic−isotropic transition during thermal heating was obtained for the biphasic and the nematic phase. (iii) No thermal hysteresis was observed for the helix−coil transitions during heating or cooling for all phases (isotropic, anisotropic, and biphasic). (iv) Departure from the Cox Merz rule for the biphasic and nematic phases was observed, with the shear rate viscosity lower from the oscillatory complex viscosity. (v) Interestingly, both isotropic and nematic phases have similar molecular weights and polydispersity indexes, as has also the biphasic sample that contains these phases. From elemental analysis, it was also found that isotropic, anisotropic, and biphasic samples all have roughly the same KC concentration and sodium iodide values.

In addition to the similarities, a number of *differences* were also observed: (i) Below the critical transition concentration (C_i), the viscosity of the isotropic solutions, obtained by the dilution of the anisotropic systems—from either the nematic phase or the biphasic phase—were *higher* than those of the isotropic solutions (the viscosity increases in the order $B_{nem} > B_{biph} > B_{iso}$). However, beyond C_i, the viscosity increases in the order $B_{iso} \gg B_{biph} \approx B_{nem}$. (ii) The steady-shear viscosity of the isotropic solutions was much less dependent on shear rate than those of liquid crystalline and biphasic solutions. Thus, the orientation of rigid rods in KC anisotropic phases due to the effect of shear contributes markedly to the viscosity changes. (iii) A characteristic property of the anisotropic phase is the increase in viscosity as the temperature was increased up to the nematic−isotropic transition. The biphasic phase due to the presence of isotropic phase has a nematic−isotropic maximum at lower temperature than the nematic phase. (iv) Anisotropic phases most probably persist up to a certain temperature (much before the helix−coil transition), and beyond that the nematic concentration decreases as the amount of helices decreases and the temperature increases. The effect of the temperature on the viscosity of the anisotropic phase of KC depends on the temperature direction from which the nematic−isotropic and the helix−coil transitions were approached. Thus, on cooling, the biphasic KC sample shows higher viscosity than the same sample on heating. This is because the volume fraction of the nematic phase strongly depends on the helical content which changes with temperature and as well on the rate at which the helix concentration increased (the cooling rate) that affects the ability of the polysaccharide to reach the equilibrium state. The helix−coil transition of KC isotropic phase is a few degrees lower than the transition of the anisotropic phases. (v) The curve of viscosity vs shear rate of a sample close to anisotropic−isotropic transition temperature has three flow regions (a first shear thinning at low shear rates, a constant viscosity region, and a final shear thinning behavior) as typically reported for other LCP's. (vi) In the KC anisotropic systems, there are important intermolecular interactions and molecular alignments of the "rigid rods" that control the rheological behavior differently than the entanglement process which occurs in the isotropic phase.

This is fully consistent with the departure from the Cox−Merz rule that anisotropic samples follow, with the viscosity changes due to the effect of shear, and with the melting behavior of KC liquid crystals.

Acknowledgment. We thank Prof. L. Piculell and Dr. G. J. Vroege for valuable discussions. We also thank Dr S. Ndoni of CPKelco for valuable help with the molecular weight determination.

Appendix

(1) Characteristics of κ-carrageenan in 0.1 M NaI: helix radius, $r_o = 7$ Å ($D = 14$ Å, from neutron and X-ray scattering); charge density, $Y = (8.2\ \text{Å})^{-1} = 0.122\ \text{Å}^{-1}$; persistence length, $P = 356$ Å; contour length, $L = 2327$ Å; Bjerrum length, $Q = 7.135$ Å; Debye length, $\kappa^{-1} = 7.577$ Å.

(2) The effective diameter: From eq 1 we derive

$$D_{\text{eff}} = D\left[1 + \frac{\ln A' + C_E + \ln 2 - {}^1/_2}{\kappa D}\right]$$

where $A' = \Pi\Gamma^2 e^{-kD}/2kQ$, Γ is a constant $= 6.39$, C_E is Euler's constant $= 0.5772....$ and D is the helix diameter (bare diameter). $D = 14$ Å in our case by taking the radius of 7 Å found by neutron scattering.

Considering that the Bjerrum length is $Q = q^2/\epsilon\, k_B T$, then

$$A' = \Pi\Gamma^2 e^{-\kappa D}/2\kappa Q = 10.724$$

and finally

$$D_{\text{eff}} = D\left[1 + \frac{\ln A' + C_E + \ln 2 - {}^1/_2}{\kappa D}\right] = 37.81\ \text{Å}$$

(3) When we substitute D_{eff} into the expression of the twisting parameter, eq 4

$$h = 1/kD_{\text{eff}} = 0.2$$

(4) Coexistence concentrations (in scaled form)

$$C_i = \frac{0.3588}{1 - \sqrt{x}}$$

and

$$C_a = \frac{C_i}{\sqrt{x}}$$

with $x = 0.8648 + 0.0991h = 0.8846$.

Thus, $C_i = 6.034$ and $C_a = 6.146$.

(5) Coexistence volume fractions

$$C_{i,a} = (\Pi/4)PLD_{\text{eff}}(N_L/V)$$

For the isotropic and the nematic phase:

$$(N_L/V)_i = \frac{C_i}{(\pi/4)PLD_{\text{eff}}} = 2.45 \times 10^{-7}\ \text{macromolecules/Å}^3$$

$$(N_L/V)_a = \frac{C_a}{(\pi/4)PLD_{\text{eff}}} = 2.5 \times 10^{-7}\ \text{macromolecules/Å}^3$$

$(N_L/V)_{i,a}$ can be also expressed in moles of polymer/L (M) by multiplying the values of $(N_L/V)_{i,a}$ by $10^{27}/6.022 \times 10^{23}$.

$$(N_L/V)_i = 4.07 \times 10^{-4}\text{mol/L} \quad \text{and}$$

$$(N_L/V)_a = 4.15 \times 10^{-4}\ \text{mol/L}$$

Finally, the isotropic and nematic concentration in wt % can be obtained by a further multiplication by the molecular weight $M_w/10$.

$$\rho_i\ (\text{wt \%}) = 4.07 \times 10^{-4} \times (115.8 \times 10^3/10) = 4.71\%$$

$$\rho_a\ (\text{wt \%}) = 4.15 \times 10^{-4} \times (115.8 \times 10^3/10) = 4.8\%$$

References and Notes

(1) Rees, D. A.; Morris, E. R.; Thom, D.; Madden, J. K. In *The polysaccharides 1*; Aspinal, G. O., Ed.; Academic Press: New York, 1982; p 195.
(2) Piculell, L. In *Food Polysaccharides and their applications*; Stephen, A. M., Ed.; Marcel Dekker Inc.: New York, 1995; p 205.
(3) Russo, P. S.; Chowdhury, A. H.; Mustafa, M. *Mater. Res. Soc., Symp. Proc.* **1988**, *134*.
(4) Borgström, J.; Quist, P.-O.; Piculell, L. *Macromolecules* **1996**, *29*, 5926.
(5) Piculell, L.; Sparrman, T.; Ramzi, M.; Borgström, J.; Quist, P.-O. *Macromolecules* **1998**, *31*, 5152.
(6) Bongaerts, K.; Reynaers, H.; Zanetti, F.; Paoletti, S. *Macromolecules* **1999**, *32*, 683.
(7) Onsager, L. *Ann. N.Y. Acad. Sci.* **1949**, *51*, 627.
(8) Flory, P. J. *Proc. R. Soc. London* **1956**, *A234*, 73.
(9) Frenkel, S. Ya. *J. Polym. Sci.* **1974**, *C44*, 49.
(10) Tanaka, F.; Stockmayer, W. *Macromolecules* **1994**, *27*, 3943.
(11) Conio, G.; Bianchi, E.; Ciferri, A.; Tealdi, A.; Aden, M. A. *Macromolecules* **1983**, *16*, 1264.
(12) Conio, G.; Bianchi, E.; Ciferri, A.; Krigbaum, W. R. *Macromolecules* **1984**, *17*, 856.
(13) Fraden, S.; Maret, G.; Caspar, D. L. D.; Meyer, R. B. *Phys. Rev. Lett.* **1989**, *63*, 2068.
(14) Suto, S. *J. Polym. Sci., Polym. Phys. Ed.* **1984**, *22*, 637.
(15) Fortin, S.; Charlet, G. *Macromolecules* **1989**, *22*, 2286.
(16) Navard, P. *J. Polym. Sci. Poly. Phys. Ed.* **1986**, *24*, 435.
(17) Milas M.; Rinaudo, M. *Polym. Bull. (Berlin)* **1983**, *10*, 271,.
(18) Allain, C.; Lecourtier, J.; Chauveteau, G. *Rheol. Acta* **1988**, *27*, 255.
(19) Inatomi, S.; Jinbo, Y.; Sato, T.; Teramoto, A. *Macromolecules* **1992**, *25*, 5013.
(20) Van, K.; Teramoto, A. *Polym. J.* **1982**, *14*, 999.
(21) Revol, J. F.; Manchessault, R. H. *Int J. Biol. Macromol.* **1993**, *15*, 329.
(22) Yanaki, T.; Norisuje, F.; Teramoto, A. *Polym. J.* **1984**, *16*, 165.
(23) Dave, V.; Sheth, M.; Mccarthy, S. P.; Ratto, J. A.; Kaplan, D. L. *Polymer* **1998**, *39*, 1139.
(24) Larez-V, C.; Crescenzi, V.; Ciferri, A. *Macromolecules* **1995**, *28*, 5280.
(25) Cuppo, F.; Reynaers, H.; Paoletti, S. *Macromolecules* **2002**, *35*, 539.
(26) Khokhlov, A. R.; Semenov, A. N. *Physica A* **1981**, *108*, 546.
(27) Vroege, G. J. *J. Chem. Phys.* **1989**, *90*, 4560.
(28) Vroege, G. J.; Odijk, T. *J. Chem. Phys.* **1987**, *87*, 4223.
(29) Stroobants, A.; Lekkerkerker, H. N. W.; Odijk, T. *Macromolecules* **1986**, *19*, 2232.
(30) Marrucci, G. In *Liquid Crystallinity in Polymers, Principles and fundamental properties*; Giferri, A., Ed.; VCH Publishers: New York, 1991; p 395.

(31) Lee, S. D.; Meyer, R. B. In *Liquid Crystallinity in Polymers, Principles and fundamental properties*; Giferri, A., Ed.; VCH Publishers: New York, 1991; p 343.
(32) Borgström, J.; Egermayer, M.; Sparrman, T.; Quist, P.-O.; Piculell, L. *Langmuir* **1998**, *14*, 4935.
(33) Morris, E. R. *Carbohydr. Polym.* **1990**, *13*, 85.
(34) Chronakis, I. S.; Doublier, J.-L.; Piculell, L. *Int J. Biol. Macrom.* **2000**, *28*, 1.
(35) Doi, M. *J. Polym. Sci., Polym. Phy. Ed.* **1981**, *19*, 229.
(36) Odijik, T. *Macromolecules* **1986**, *19*, 2313.
(37) Papkov, S. P.; Kulichikhin, V. G.; Kalmykova, V. D.; Yamackin, A. *J. Polym. Sci., Polym. Phys. Ed.* **1974**, *12*, 1753.
(38) Kiss, G.; Porter, R. S. *J. Polym. Sci., Polym. Symp.* **1978**, *65*, 193.
(39) Kiss, G.; Porter, R. S. *Mol. Cryst. Liq. Cryst.* **1980**, *60*, 267.
(40) Robinson, J. C.; Ward, R.; Beevers, B. *Discuss Faraday Soc.* **1958**, *25*, 29.
(41) Onogi, S.; Asada, T. In *Rheology*; Astarita, G., Marrucci, G. Nicolais, I., Eds.; Plenum Press: New York, 1980; Vol. I, p 127.
(42) Walker, L.; Wagner, N. *J. Rheol.* **1994**, *38*, 1525.
(43) Wisssbrun, K. F. *Faraday Discuss., Chem. Soc.* **1985**, *79*, 161.
(44) Grizzuti, N.; Moldenaers, P.; Mortier, M.; Mewis, J. *Rheol. Acta* **1993**, *32*, 218.
(45) Grizzuti, N.; Cavella, S.; Cicarelli, P. *J. Rheol.* **1990**, *34*, 1293.
(46) Aoki, H.; White, J. L.; Fellers, J. F. *J. Appl. Polym., Sci.* **1979**, *23*, 2293.
(47) Oertel, R.; Kulicke, W.-M. *Rheol. Acta* **1991**, *30*, 140.
(48) Chronakis, I. S.; Piculell, L.; Borgström, J. *Carbohydr. Polym.* **1996**, *31*, 215.
(49) Ramzi, M.; Borgström, J.; Piculell, L. *Macromolecules* **1999**, *32*, 2250.
(50) Carnali, J. O. *J. Appl. Polym. Sci.* **1991**, *43*, 929.
(51) Matheson, R. R. *Macromolecules* **1980**, *13*, 643.

BM020015K